Review Article

Imaging the young adult hip in the future

Vasco V. Mascarenhas[1], António Caetano[2]

[1]MSK Imaging Center (UIME), Hospital da Luz, Lisboa, Portugal; [2]Radiology Department, Hospital Curry Cabral, Lisboa, Portugal

Contributions: (I) Conception and design: All authors; (II) Administrative support: All authors; (III) Provision of study materials or patients: All authors; (IV) Collection and assembly of data: All authors; (V) Data analysis and interpretation: All authors; (VI) Manuscript writing: All authors; (VII) Final approval of manuscript: All authors.

Correspondence to: Vasco V. Mascarenhas. MSK imaging center (UIME), Hospital da Luz, Av. Lusiada 100, 1500-650 Lisboa, Portugal.
Email: mascarenhas.vasco@gmail.com.

Abstract: The past fifty years have transformed diagnostic imaging of the hip joint. Innovation has been the catalyst for the transformation of radiology, as the arrival of new imaging modalities and the introduction of magnetic resonance imaging, resulted in a paradigm shift from bone morphology analysis to integrated soft tissue, joint and cartilage assessment. Hip pathology in general and the concept of femoroacetabular impingement (FAI) has come to the forefront of imaging and orthopedics. In just a few years, MRI findings that were in the past ascribed to degenerative change or normal variation must now be integrated in different entities, such as cam impingement or subspine impingement. Understanding the pathophysiology through the visualization of osseous structures and detailed depiction of soft tissue structures has become part of routine clinical imaging and has had a major impact on therapeutic decision-making. The purpose of this article is to provide a historical perspective on the utility of various types of imaging techniques for the hip joint, including cutting-edge clinical applications and topics at the forefront of musculoskeletal research. The current limitations as well as future directions of biochemical imaging will be outlined. Finally, emerging trends that will shape the field of hip imaging in the years to come will be discussed.

Keywords: Hip; imaging; femoroacetabular impingement (FAI); magnetic resonance

Received: 23 February 2018; Accepted: 20 April 2018; Published: 26 May 2018.
doi: 10.21037/aoj.2018.04.10
View this article at: http://dx.doi.org/10.21037/aoj.2018.04.10

Introduction

Musculoskeletal (MSK) imaging has undergone a major transformation over the past five decades. Advancements in orthopaedic surgery and arthroscopy have developed in unison with imaging techniques, which has led to improvements in clinical diagnosis, therapeutic interventions and patient prognostication.

With recent major developments of magnetic resonance imaging (MRI), attention has turned to the unique capability of defining bone morphology and soft tissue abnormalities. Additionally, the development of state-of-the-art quantitative MRI techniques has allowed for the depiction of early stage cartilage lesions (1). However, MRI is still limited in its ability to provide static morphological diagnosis. In the future, we will likely see all-in-one patient-centric examinations based on MRI, which can provide valuable information on joint morphology, biochemical function and dynamic "*in vivo*" assessment.

Imaging

The past

Conventional radiography (XR) remains the cornerstone of hip imaging (2), and continues to have a role in screening, diagnosis and post-operative surveillance. The advent of computed tomography (CT), represented a transformation in clinical practice from XR to cross-sectional imaging. Initially, only low-quality axial two-dimensional images were available and examination times were even longer than current MRI acquisition times. Only with the establishment

Table 1 Timeline of major achievements in imaging and hip orthopedics

Timeline	Authors	Findings or procedure	Event
1933	Elmslie (4)	"many patients who develop OA at a comparatively early age – for example from 40 to 50- will be found to have a pre-existing deformity of the joint"	Landmark on research to determine the cause of hip OA
1958	Wiles (5)	Precedent of the modern genre arthroplasties	First prosthetic total hip replacement
1965	Murray (6)	Concept that secondary OA also derives from cases with subtler morphologic hip deformities. OA secondary to the "tilt deformity"	OA described as secondary if associated to a pre-existing deformity
1974	Ambrose and Hounsfield (7,8)	The first description of a Computerized axial tomography in the radiology literature by Hounsfield and colleagues in the British Journal of Medicine	First clinical application of computerized axial tomography
1975	Murray and Stulberg (6,9)	"pistol grip deformity" first described as a finding similar to the "tilt deformity", including a flattened lateral femoral neck with widening and shortening of the FHN	Cam deformity first described
1976	Mansfield (10)	Finger image of the Dr. Maudsley	First-ever human MRI image
1987	Hajek (11)	To enhance the efficacy of MRI in evaluating articular soft-tissue structures, arthrography was performed before imaging in 45 fresh cadaveric specimens	First study of direct magnetic resonance arthrography with gadopentetate dimeglumine/saline mixture into cadaveric shoulder joints
1993	Langen (12)	Image quality improved with substantial radiation dose reduction	Introduction of digital radiography
1998	–	Simultaneous acquisition of four interweaving helices or spiral paths where previously there had been only one had a profound effect on the volume and spatial resolution of imaging	First multidetector (four-detector row) scanner CT
2001	Ganz (13)	Safe hip surgical dislocation	Understanding the pathophysiology of FAI

FHN, femoral head-neck; OA, osteoarthritis.

of multiplanar reconstructions based on 3D data sets was the use of CT in MSK imaging transformed (3), allowing for accurate and improved surgical planning (*Table 1*).

MRI allows for a more comprehensive analysis of the articular cartilage, capsulolabral tissue, soft-tissue and osseous structures (14). Thirty years ago, MRI examinations were technically difficult and resulted in low resolution images. The development of MR arthrography (MRA) had a major impact on treatment decisions, particularly in the evaluation of cartilage and labral integrity (2). In the mid-1990s MRA was the examination of choice for the evaluation of labral disruption, and remains the imaging gold-standard for patients with femoroacetabular impingement (FAI) (15).

The present

The hip joint has gained particular attention in the last decade in parallel with significant advances in MSK imaging. Ganz developed a revolutionary technique that allowed for safe dislocation of the hip and direct visualization of the joint, which provided fundamental insights into the pathogenesis of early osteoarthritis (OA) (3,13). New biomechanical concepts were recognized such as the depiction of FAI as a major cause of secondary OA in non-dysplastic hips (14-18).

Crucial questions still remain to be answered. For instance:

(I) What morphological factors, beside cam-type FAI and dysplasia contribute to hip OA (19)?
(II) During disease progression, what is the exact discriminative point when cartilage damage becomes irreversible (20)?
(III) Why are some patients with FAI morphology asymptomatic and never develop OA (21-23)?

Accurately determining the amount of articular cartilage injury is important as it has a direct impact on the clinical decision-making between hip preservation surgery and total hip replacement (24). The workup of the young patient with hip pain generally follows specific algorithms (25)

(*Figures 1,2*). The primary goals of diagnostic imaging are to accurately identify osseous morphology and characterize the amount of chondrolabral damage. However, it is important to understand the limitations and strengths of each imaging modality, as for example, both XR and CT lack accuracy for assessing articular cartilage pathology (2), whereas specific MRI sequences and advanced technologies can be useful (26).

New technical and imaging innovations are presently available in routine clinical setting, bringing important implications to the study of the young hip (21). The diagnostic performance of these techniques may therefore improve the ability to predict an individual patient-specific outcome (2,22).

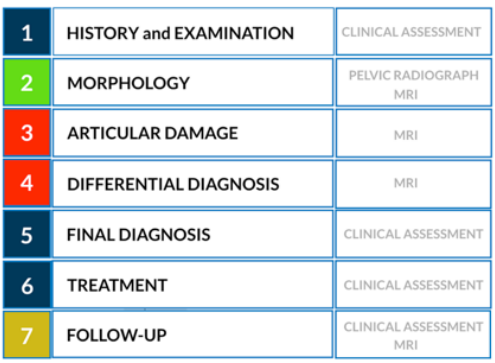

Figure 1 Algorithm for evaluation of FAI used at Hospital da Luz in Lisbon. First, the diagnosis of FAI is suspected based on patient history and clinical findings. Next, the hip is assessed on an anteroposterior pelvic radiograph (acetabulum and pincer morphology) and on a 45° Dunn view. Using MRI, the morphology of the femur is assessed (cam deformities, femoral torsion) and damage to the cartilage and labrum is evaluated. Lastly, all data are combined to reach a diagnosis, define appropriate course of treatment and follow-up.

Radiography

After history and clinical examination, XR is useful to assess for OA, including evaluation of bone morphology, joint space width as well as to exclude other hip pathology (23). XR should include a standing anteroposterior (AP) view of the pelvis, and a lateral view of the affected hip. Nonetheless the utility and accuracy of the various types of radiographs remains controversial (25,27).

Ultrasound, arthrography and CT

Conventional arthrography is seldomly performed as it has been replaced by MRA. However, the origin of the referred hip pain might still be confirmed by intra-articular anesthetic injection (28). Ultrasound is not routinely used in the workup of FAI, although ultrasound-guided injection procedures can be helpful to exclude pain derived from periarticular structures such as trochanteric pathology, iliopsoas bursitis and other myotendinous elements (29). CT can be helpful in the characterization of fractures and unusual bony anatomy. Further, it is helpful to evaluate bony morphology of the pelvis, version, the anterior inferior iliac spine and extra-articular causes of impingement, as well as, building 3D models (30-32). Regarding FAI, pincer-type morphology is currently well addressed with standard

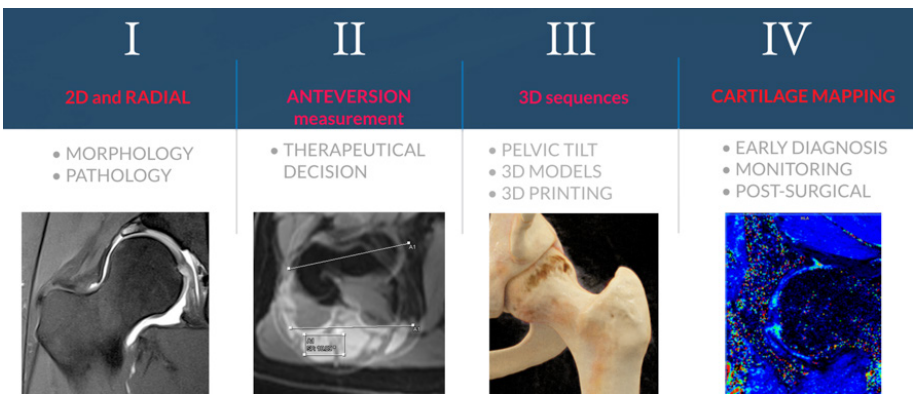

Figure 2 Schematic figure representing proposed complete MRI protocol for the assessment of the young hip. 2D sequences with radial imaging are used for the assessment of morphology and pathology. Version assessment of the femoral neck is performed. 3D sequences to allow for correction of pelvic tilting, 3D modelling, 3D printing and virtual ROM simulations. Finally, a sequence that allows for cartilage biochemical mapping.

pelvic XR (25), while for cam morphology, CT or MRI can offer a clear advantage since the complexity of the three-dimensional femoral shape can be thoroughly evaluated (33). Furthermore, measuring femoral version is only feasible with cross-sectional imaging (25).

Magnetic resonance imaging

MRI is an all-in-one imaging method as it depicts joint and periarticular pathology, including stress fractures, myotendinous injuries, bursitis and signs of ischiofemoral impingement (26). MRI can accurately assess bone morphology associated with FAI syndrome and detect chondrolabral damage. While conventional MRI can only detect macroscopic chondral damage (34), the presence of subchondral edema and cystic changes, have been shown to be indirect signs of advanced cartilage changes in the hip joint at the time of arthroscopy (35).

MRI techniques include (23,36):

(I) Conventional MRI;
(II) Magnetic resonance arthrography (direct/indirect; with or without traction);
(III) Quantitative biochemical MRI: T2/T2* mapping, delayed gadolinium-enhanced of cartilage (dGEMRIC) and T1rho (T1ρ).

Technical advances in MSK MRI are emerging with potential for implementation into clinical practice, namely (37,38):

(I) High-resolution 3D sequences for imaging of cartilage (23);
(II) Biochemical imaging of cartilage;
(III) 7.0 Tesla MRI (39);
(IV) Imaging of metal prosthetics with novel MRI pulse sequences (22).

New quantitative MRI imaging is encouraging for early detection of chondral and labrum injuries (40), as it probes changes in cartilage properties and biochemical composition, which represents an early stage of the degenerative cascade (41).

High-Resolution MRI

In order to obtain high-resolution MRI, a compromise between time and resolution is mandatory given that technical details are optimized (42,43). As such, some factors must be warranted:

(I) Time: maintain patient throughput with short examination times (around 30 minutes);
(II) Magnet: 3.0Tesla MRI has been widely adopted for hip evaluation. The theoretical doubling of signal-to-noise ratio can be used to obtain high-resolution (hR) imaging and/or shorter scan acquisition times;
(III) Coils: dedicated hip coils for optimal image quality (44). Improved coil geometry will further improve image quality;
(IV) Advanced morphological sequences (37):
- ❖ Implementation of parallel imaging allowing scan time to be accelerated;
- ❖ Compressed sensing;
- ❖ Isotropic MR images allowing for multiplanar reformats and 3D imaging.

MR arthrography

MRA can be performed by introduction of contrast material either (I) intra-articularly, as in direct MRA (dirMRA) or (II) intravenously, as in indirect MRA (indMRA) (45).

A detailed and comprehensive protocol for dirMRA should be strictly followed to achieve maximum quality (*Figures 2-6*). MRA of the hip plays a major role in:

(I) Diagnosing internal derangements of the joint (46);
(II) Evaluating symptomatic improvement following administration of anesthetic, helpful to confirm that symptoms and joint changes are related.

Several studies have compared the performance of these different protocols with variably reported accuracies (47-49). Previously, MRA has shown to be more accurate in detecting minor acetabular cartilage defects than non-contrast MRI (50,51). Diagnostic test accuracy was shown to be better for dirMRA when compared with conventional MRI for detection of labral and cartilage injury, in specific chondral lesions. Concerning indMRA, good results were also obtained, although more studies are needed to fully assess its accuracy (52). In patients with suspected FAI, MRA may still be considered the gold standard of imaging for the evaluation of the chondrolabral injury (25,49,53).

MR arthrography with leg traction

The rationale behind traction MRA (traMRA) is centered on the separation of the acetabular and femoral surfaces allowing a better assessment of the chondrolabral interface and central compartment (54,55). Recently, a study correlating traMRA with arthroscopy assessed the utility of this technique for the diagnosis of chondrolabral damage (55). Traction was well tolerated by most patients and consistently achieved separation of cartilage layers, enabling accurate detection of chondral and labral lesions (55).

Procedure: prior to the application of traction with the hip slightly flexed, a conventional arthrography injection

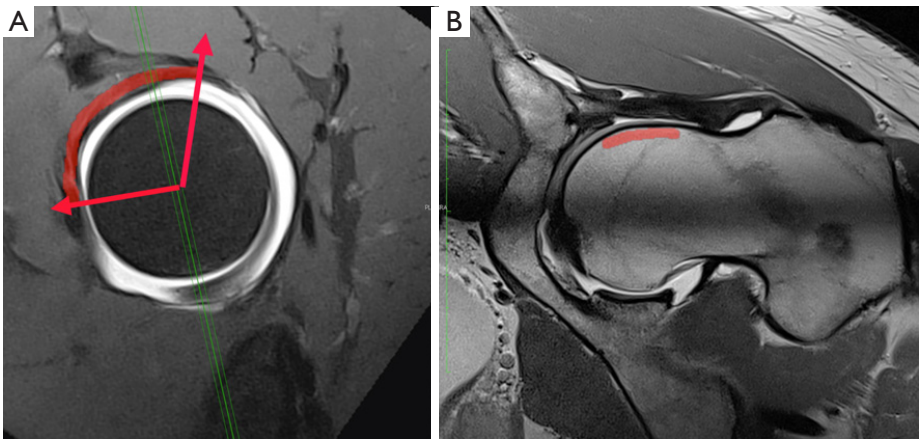

Figure 3 Direct arthro-magnetic resonance examination. Sagittal fat-suppressed proton-density sequence (A) and corresponding radial cut in Proton-Density (B). Red curved line represents CAM morphology assessed on the radial cut at 1:00 o'clock (B) and corresponding deformity in the sagittal plane extending from 11:30 to 3:00.

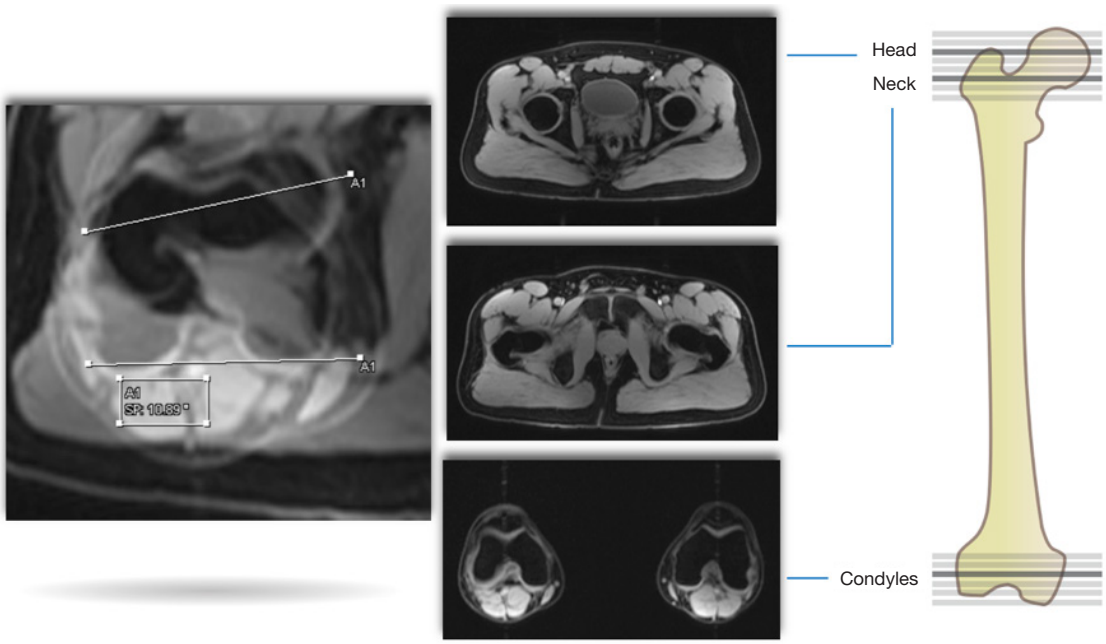

Figure 4 Measuring femoral torsion by MRI as a routine part of general hip workup. Femoral version is determined by the angle between the femoral neck axis and an axis parallel to the posterior aspect of the femoral condyles, measured in the transverse plane.

(10–27 mL) is performed and MR-compatible traction devices are routinely used for continuous traction during the examination. Traction devices consist of a weight connected to a pulley system, a cable or rope connected to the leg either with an ankle brace or with adhesive straps for skin traction. The amount of traction varies between 6 and 23 kg for a period ranging between 3 and 19 min among different studies (51,54,55).

Schmaranzer *et al.* (55) reported detection of acetabular/femoral chondral injury with a sensitivity of 85–88%/81–86% and specificity of 78–96%/91–94%, respectively (*Table 2*). The combination of contrast agent and additional space from distraction allows for improved visualization of the cartilage surfaces of the femoral head and acetabulum as

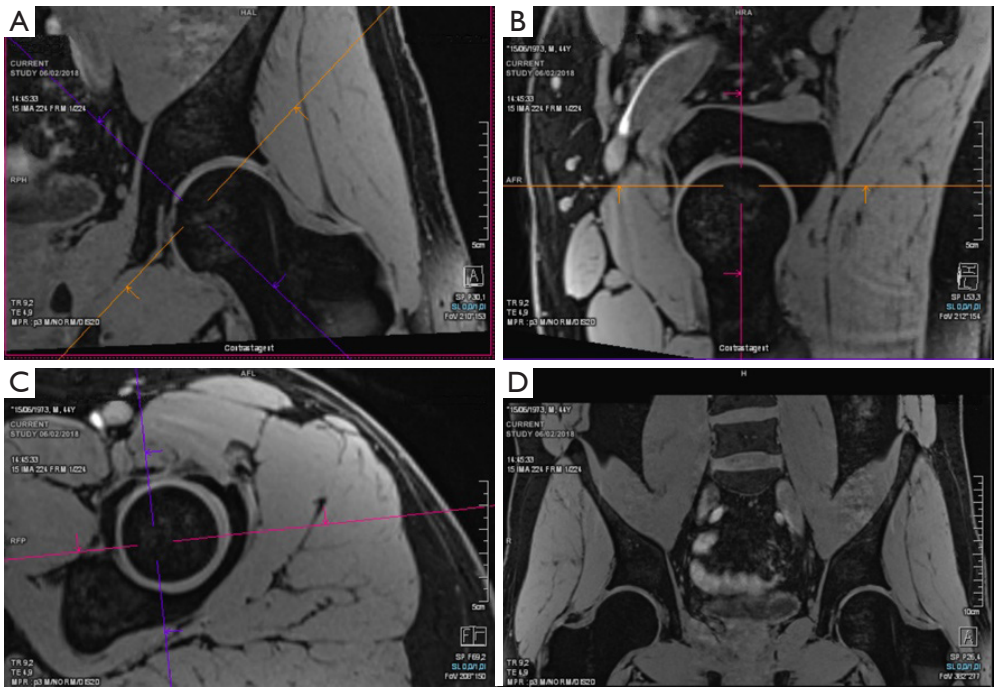

Figure 5 A 44-year-old male undergoing hip preserving surgery. Multiplanar reformats based on isotropic T1-VIBE sequence of the whole pelvis. (A) Coronal reformat of the hip. A Cam morphology is depicted on the transition of the superior quadrants with an intact chondrolabral junction; (B) oblique axial reformat (long axis of the neck), showing normal offset of the femoral head-neck junction; (C) short neck axis reformat; (D) coronal pelvic reformat.

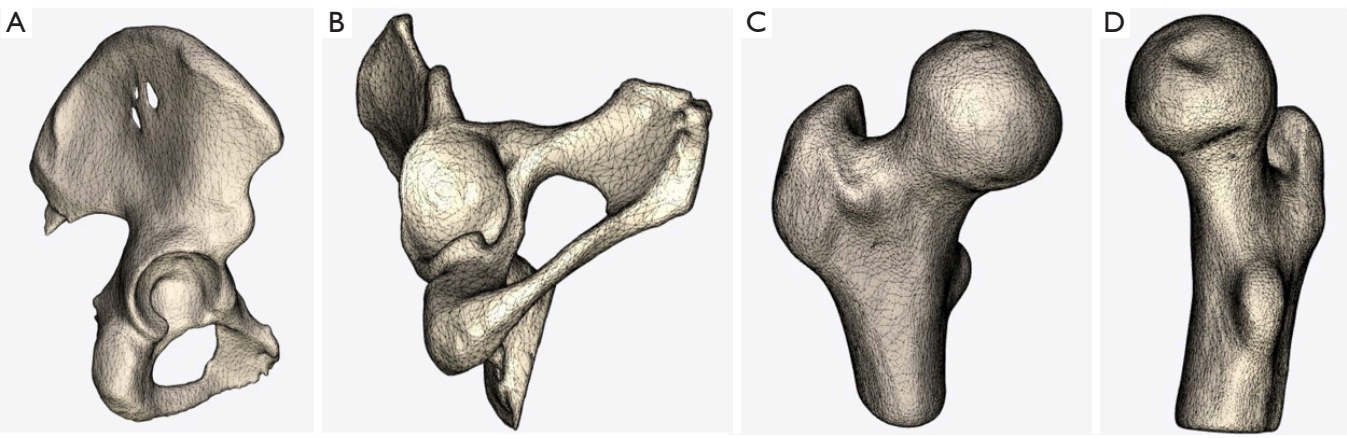

Figure 6 A 23-year-old female undergoing hip preserving surgery. 3D Model reconstructed based on volumetric MRI sequence of the pelvis. (A) Lateral view of the acetabulum; (B) inferior view of the acetabulum, showing normal pelvic morphology; (C) femoral 3D model anterosuperior view, showing discrete convexity of the femoral head neck junction; (D) medial view of the same model.

Table 2 Sensitivity and specificity for detection of chondral damage according to different studies using magnetic resonance

MRI techniques	Sensitivity (%)	Specificity (%)
MRA (53,56,57)	40–83	41–91
MRA with traction (55)	81–88	78–96

distinct entities.

Advanced cartilage imaging

Improved evaluation of articular cartilage status is imperative to allow both assessment of patients who may benefit from FAI surgery, as well as, long-term evaluation of clinical outcomes (26). Recognition of pre-existing degenerative changes at an early stage is therefore crucial. Although large defects can be confidently detected by conventional MRI, morphologic sequences lack crucial (quantitative) information on the pathophysiology of cartilage degeneration (36). Prior to structural damage of the cartilage, early changes can be evaluated using functional MRI techniques (1). This field remains an ongoing subject of research and future developments are necessary to allow its widespread use (1). Currently the main limitations include the narrow applicability of normative threshold standards (as they are dependent on multiple factors) and current indefinite clinical correlation. Challenges in quantitative imaging (17,23,41,58) presently include:

(I) Hardware related:
  (i) Need for dedicated cartilage-specific sequences and high-MR field strengths;
  (ii) High signal-to-noise (SNR) ratio and high-spatial resolution;
  (iii) Technical variations (changes in acquisition parameters can lead to limited comparability).

(II) Anatomy related:
  (i) Hip joint cartilage (deep location, thickness and its spherical shape);
  (ii) Hip susceptibility to artifacts and volume averaging;
  (iii) Mapping values represent the sum of the signal of joint fluid and both chondral surfaces;
  (iv) Standard regional/sectorial differences in the biochemical composition of hip cartilage.

(III) Patient related:
  (i) Cartilage loading (has an influence on the extracellular matrix). Current recommendation is that this technique should be performed in the unloaded state at the end of the MR scan;
  (ii) Inter-subject anatomic variations (can lead to misinterpretations with added limited comparability; patient-driven normalization can compensate for deviations caused by technical changes and variations related to age and individual cartilage configuration).

Quantitative MRI techniques (1) can probe the depletion and/or disorganization of proteoglycan and collagen/water (*Table 3*):

Delayed gadolinium-enhanced MRI of cartilage (dGEMRIC)

Glycosaminoglycan (GAG) are negatively charged polysaccharides (consist of NH and OH groups) that highly attract water and serve to resist compressive forces. High contents are found in the extracellular matrix of healthy cartilage (1). The dGEMRIC is used for assessing typical features of early-onset OA, namely GAG loss and collagen breakdown (41). It is based on the use of a contrast agent named gadopentetate dimeglumine [$Gd(DTPA)^{2}$]. $Gd(DTPA)^{2-}$ is an anionic molecule and is negatively charged. In the case of depletion of GAGs due to arthritis, these GAG's are replaced by $Gd(DTPA)^{2-}$ within the cartilage if given time. Consequently, the measurable $Gd(DTPA)^{2-}$ concentration is relatively low in native cartilage and relatively high in case of arthritis. The distribution of $Gd(DTPA)^{2-}$ in the cartilage can be measured by a T1 weighted sequence. By measuring the spatial variations between $Gd(DTPA)^{2-}$ and GAGs, the quality of cartilage can be determined (75,76).

This technique can either be used with direct intra-articular or intravenous injection of a contrast agent (75), and a time delay separating contrast agent administration and image acquisition is used (intravenous: 30–90 min; intra-articular: 15–30 min) (76). The most widely used protocol of Burstein recommends 10–20 minutes of exercise (e.g., walking, climbing stairs, and cycling) immediately after the contrast administration. No exercise is recommended after intra-articular based protocol. It has been suggested that isolated T1Gd assessment of the hip joint cartilage is sufficient for the evaluation without the need for time consuming pre-contrast imaging (except in the setting of post-operative cartilage repair) (77). Baseline dGEMRIC was shown to be able to predict the development of radiographic OA (40). Similarly, the size and position of cam morphology determined the severity and location of progressive cartilage damage, supporting the

Table 3 Main characteristics of MRI compositional techniques

Technique	Target	Sequences	Normal	Pathology	Pros	Cons
dGEMRIC (34,59-63)	Cartilage GAGs (concentration of negatively charged contrast molecules of Gd-DTPA is inversely proportional to the local proteoglycan concentration)	Intravenous or direct intra-articular application of contrast agent. T1 weighted sequence. Time frame between contrast agent administration and T1Gd relaxation time measurement	Higher T1Gd values toward the superior zone reflecting a high-GAG concentration at this weight-bearing region	Higher T1Gd relaxation time values will be measured in healthier cartilage, whereas low T1Gd values will be observed in degenerated, GAG-depleted cartilage. Lower T1Gd values in asymptomatic hips with cam deformities compared with morphologically normal hips. Severity of the GAG loss correlates with the magnitude of the cam deformity	Most studied and standardized methods Effectiveness in histological and biochemical evaluation of repair tissue at early stage after allograft chondrocyte implantation. May predict development of OA	2D-based technique. Longer acquisition time. Risk of motion artifacts. Regional differences in GAG concentration. Pharmacokinetic-related contrast agent uptake variations owed to age, sex, body
T1 ρ (64-66)	GAG (sensitive to the protons of hydrogen molecules attached to proteoglycans in the extracellular matrix)	"Spin lock" pulses to lock the transverse magnetization and drive the recovery of longitudinal magnetization	T1ρ relaxation time is inversely correlated with the GAG content in cartilage regions with normal T2 relaxation time	T1ρ values are increased with progressive joint degeneration	Seems to be more sensitive for the detection of early cartilage degeneration than T2 mapping. Does not require contrast. No time frame between contrast agent and MRI	Involves high-RF energy which can result in tissue heating. May not be specific to any one inherent tissue parameter, as concentration of other molecules beside collagen fibers produce changes in T1ρ values. Not commercially available and still requires post-processing. SNR ratio constraints associated with the thin cartilage layers and hip deeper location. Application in the hip joint relatively limited due to SNR constraints
T2 mapping (67-69)	Collagen and Water (sensitive to collagen and water content and collagen fiber orientation in the extracellular matrix)	Multi-echo spin-echo sequences	T2 values decrease progressively from surface layer to deep layer (because of anisotropy in different layers)	Damage to the extracellular matrix is associated with increased T2 relaxation times. Normal cartilage T2 gradient pattern becomes less apparent (pre-arthritic patients) or disappeared (early-arthritic patients)	Easy to implement. No contrast agent. No time frame needed. Well documented reproducibility and validity of T2 quantification	Long-acquisition times that typically exceed 10 min. Constraint on 2D acquisitions (magic angle effect). Less sensitive for detecting early stages of cartilage lesions. High degree of structural variation of the cartilage tissue with respect to location of the joint

Table 3 (*continued*)

Table 3 (*continued*)

Technique	Target	Sequences	Normal	Pathology	Pros	Cons
T2* mapping (70-74)	Collagen and water (bulk water content and interactions between water molecules and collagen fibers within cartilage)	Multi-echo gradient-echo sequences	Higher values in superficial zone (due to high-water content and superior molecule mobility), and lower T2* values in the cartilage-bone interface. Topographical T2* variations (low values posterior-superior and anterior-inferior at the periphery of the acetabulum)	Negative correlation between the histological grading of degenerated cartilage (Mankin grading) and T2*. Correlated T2* maps of acetabular cartilage (superficial, deep, and full-thickness cartilage) with intra-operative arthroscopic cartilage assessment (cartilage degeneration grading according to a modified Beck scale). Lower T2* values were noted for superficial, deep, and full-thickness cartilage in regions with intra- operatively identified cartilage damage	Easy to implement in clinical routine. Shorter acquisition times and higher resolution compared to T2 mapping. Ability to carry out isotropic 3D cartilage evaluation. Ultrashort echo-time enhanced T2* mapping of cartilage has the potential to visualize deep cartilage characteristics better than standard T2 mapping	Magic angle effects. Not fully validated for clinical diagnostics. More susceptible to artefact (Difficult mapping of articular cartilage in postoperative studies)

biomechanical etiology of FAI (18,78).

T2 and T2* mapping (*Figures 7,8*)

T2/T2* mapping have been shown to correlate with chondral matrix hydration and collagen integrity (1). Each tissue has a similar transverse relaxation time (T2) at a specified MR strength. Relaxation times are correlated to the speed by which nuclei lose phase after magnetic excitation. An additional de-phasing effect comes into play if gradient-echo MRI is performed, referred to as T2* mapping. T2 mapping is a well proven imaging modality (79). However, the orientation of collagen fibres influences the estimation of T2 relaxation values and reduces the accuracy of T2 mapping in certain regions of articular cartilage (magic angle effect). Due to the magic angle effect, T2 values of cartilage are influenced by its orientation relative to the static magnetic field (B0). Secondly, the acquisition times are relatively long. Thirdly, T2 mapping appears less sensitive for detecting early stages of cartilage lesions (80). T2* mapping has shorter acquisition times and higher resolution compared to T2 mapping although it is more prone to magic angle effects and is more susceptible to artifact (70).

T1ρ (T1 rho)

Similar to dGEMRIC, T1rho (T1ρ) relaxation time mapping is sensitive to the GAG content of hyaline cartilage. In a T1ρ sequence the spins in the direction of the B0 magnetization are first flipped into the transverse plane by a 90-degree radiofrequency (RF) pulse. A second RF pulse, better known as spin-lock pulse, is applied parallel to the magnetization vector. This spin-locked magnetization will relax with a time constant T1ρ and is dependent on the frequency and duration of the spin-lock pulse (TSL). The spin-lock pulse is applied with variable TSLs, at least two, at certain intervals which are also depended on the spin-lock frequency.

T1ρ—like T2 mapping—is founded on the motion of water molecules. T1ρ is widely considered to be sensitive to the protons of hydrogen molecules attached to proteoglycans of cartilage due to the second spin-lock pulse (64). Nevertheless, correlation with other factors, such as extracellular matrix, collagen content and collagen orientation were found too. The general consensus is that T1ρ may provide an imaging biomarker for the detection of cartilage degradation, based on the tissue's macromolecular content (41). In the FAI setting, it has been shown that early femoral and acetabular chondral changes can be detected before macroscopic lesions are apparent, and displays differences in distribution patterns across the deeper and

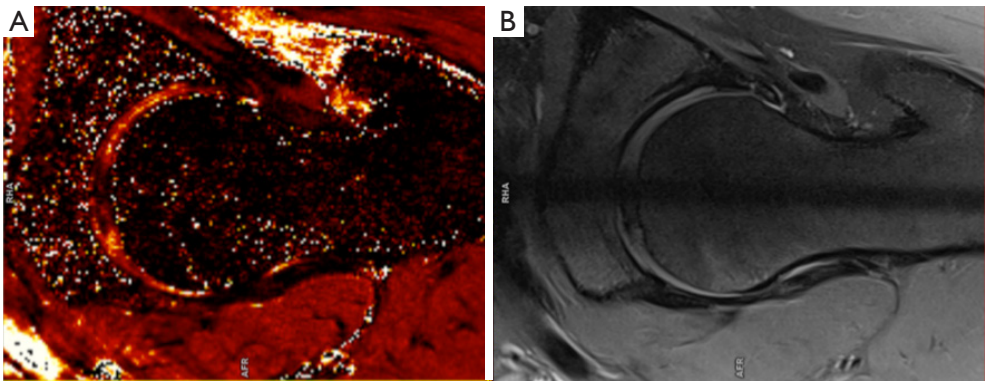

Figure 7 Pre-operative imaging of a 35-year-old female with mixed type FAI. (A) Radial T2 mapping measurements at 3.0 Tesla show decreased T2 relaxation times in the central compartment; (B) on the corresponding proton density radial cut morphological sequence, no obvious cartilage lesions are depicted.

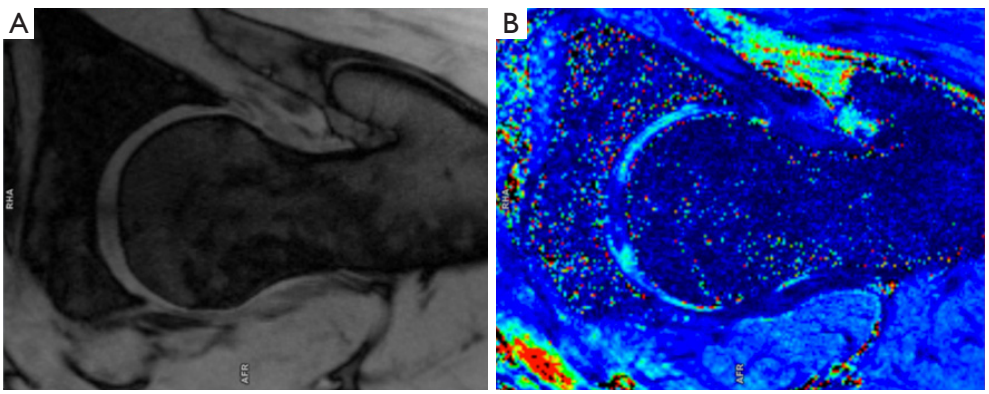

Figure 8 Pre-operative imaging of a 25-year-old male with CAM type FAI. (A) T2* radial cut morphological sequence; (B) radial T2* mapping measurements at 3.0 Tesla show decreased T2* relaxation times in the central compartment.

superficial cartilage layers (64,81).

gagCEST

gagCEST has been used in the knee joint and conceptually is the only technique that directly measures GAG cartilage content (82). It is based on an asymmetry in the z-spectrum of cartilage created by hydroxyl groups in the GAG molecule. The application of this method in the hip has not yet been demonstrated.

Sodium

Sodium (^{23}Na) cartilage imaging can be also performed in this setting. The rationale behind its use centers on the negatively charged GAG molecules in the cartilage binding of positively charged Na^+ maintaining the electroneutrality of the extracellular matrix (83). Na molecules conceptually distribute in proportion to the GAG molecules in degenerated articular cartilage. As such, proteoglycan cartilage loss caused by cartilage degeneration can be visualized (84). 3D-Isotropic MRI mapping sodium using a 7.0 Tesla system was used for the assessment of the knee, showing promise as a feasible alternative for evaluating OA (39). Limitations of sodium mapping include the need for a high-field MRI and dedicated hardware as well as anatomical constraints due to the deep location of the hip chondral surfaces.

Near future perspectives

Knowledge of biomechanics and physiopathology of the hip evolves in parallel with the need for non-invasive strategies to further assess the joint. As such, it is imperative for simultaneous advances in both static and dynamic automated imaging techniques. Currently, the acquisition

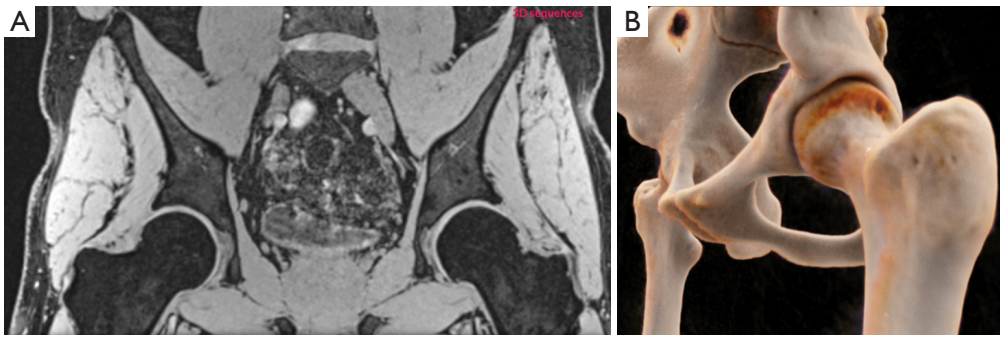

Figure 9 A 25-year-old female with hip pain undergoing MRI work-up examination, showing discrete osteophytes of the left femoral head. (A) Coronal volumetric MRI based sequence; (B) corresponding 3D Model with cinematic rendering quality.

of XR and MRA are the cornerstone of hip imaging. Computer-assisted (CompAssist) techniques have been based on data derived from isotropic CT images, while some studies based segmentation of those datasets on alternative tools such as MRI (85,86). However, MRI-based automated segmentation (AutSeg) has not yet reached the clinical standard due to relatively low contrast differences between bone and soft tissues (85).

The ideal future gold standard comprehensive all-in-one examination would comprise (23,87,88):

(I) Tools for accurate diagnosis and cartilage mapping;
(II) Pre-operative treatment planning and virtual treatment performance;
(III) AutSeg algorithms as well as intra-operative non-invasive registration methods such as statistical shape models (SM);
(IV) Intra-operative navigation (OpNav).

Developing OpNav tools to execute the pre-operative plan is currently a focus of expanding research, which has already seen clinical applications in hip and knee arthroplasty. These advances will hopefully lead to improved accuracy of intra-operative decision-making for both open and arthroscopic FAI procedures (89-91).

3D modeling (Figure 9)

Traditionally, surgeons have relied on 2D imaging to pre-operatively assess the hip, before evaluating areas of impingement by means of intra-operative dynamic visualization and fluoroscopy. However, subject-tailored surgical planning is developing on the basis of 3D hip modeling (92).

Patients with FAI have abnormal complex 3D bone and soft-tissues morphology. As such, routine 3D modeling may provide the surgeon a better understanding of the abnormal bony pathomorphology that would otherwise be difficult to visualize on 2D images. Models based on biplanar (92), 3D CT (30) or MRI (93) data sets (*Figure 9*) have been used to simulate specific individual bone morphology, define impingement-free range of motion (ROM), and to perform virtual functional analysis with different degrees of function (88). However, further clinical applicability and validation of these models for clinical diagnostics is still needed.

Automated image analysis

Most of the previous AutSeg work has been performed using XR (92) or CT (94-96). Advances in image processing have helped automate measurements, as well as, bone segmentation, thereby improving objectivity and reproducibility. Adding 3D anatomical information to the AutSeg (97) may be useful in reaching better imaging results that are less dependent on other parameters such as patient positioning.

MR imaging enables noninvasive, all-in-one, 3D assessment of the joint structure including biochemical changes with no ionizing radiation and optimal soft tissue contrast. Automated analysis using MR image sets (*Figure 10*) includes (85):

(I) An SM-based algorithm allows building 3D femoral and acetabular reconstructions;
(II) A coordinate system of the joint is generated to build a 2D shape map to project femoral head sphericity for calculation of specific parameters (for instance alpha angles);
(III) Automatically reformatted images using the constructed coordinate system;

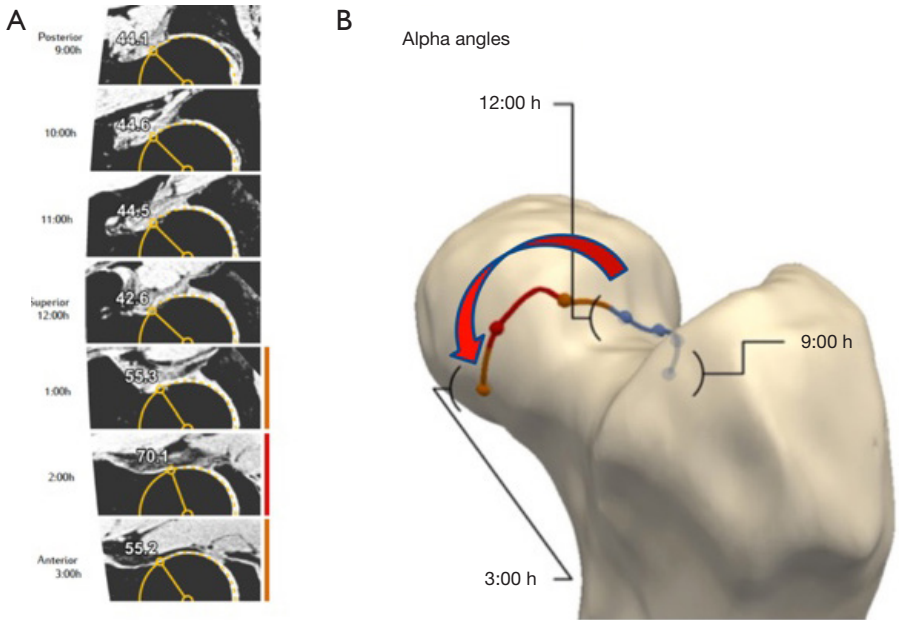

Figure 10 Volumetric semi-automated MR evaluation of the femoral head-neck junction with corresponding 3D model. (A) Automated alpha-angle (α°) measurements made at different points around the femoral head-neck junction in steps of 1° starting at 9 o'clock (posterior); 10, 11, and 12 o'clock (superior); and 1, 2, and 3 o'clock (anterior) (B). 3D Hip model (showing extension and location of a cam lesion represented on the corresponding 3D model (red arrow). Red and orange lines correspond to abnormal α°s; blue line represent normal α°s for a given α threshold.

(IV) Automated evaluation of desired parameters according to specified algorithm (*Figure 10*).

Advantages of 3D method analyzed MR images of the hip joint include (85,96,98):

(I) Allows for large-scale morphometric and clinical MR investigations of the hip region;
(II) High reliability and reproducibility;
(III) Improved analyses of cam-type morphology.

Imaging-based dynamic ROM simulations and virtual surgery

3D data sets of volumetric imaging bear high potential for the dynamic assessment of FAI allowing to perform pre-operative simulation of ROM, collision detection and accurate visualization of impingement areas. In addition to virtual 3D reconstruction of the hip joint, dynamic manipulation of the image may be useful to the surgeon, when pre-operatively assessing the deformity and planning for surgical correction (90) (*Figure 11*).

(I) "HipMotion" (86) constructs 3D representations of the femur and pelvis from CT. In addition, the model can be manipulated by the user, and pre-operative virtual ROM for patients with FAI can be calculated based on contact or interference occurring at the point of impingement.
(II) 3D software package Mimics (94) (Materialise, NV, Heverlee, Belgium). Automated morphologic analysis of the cam lesion can be conducted by MATLAB (Math Works, Natick, MA) and used to measure the clinical ROM of the hip joint. Measured motions are imposed on the 3D reconstructed anatomy, and the size and location of the abutting portion of the cam lesion are defined for each motion.
(III) "Dionics PLAN Hip Impingement Planning System" (Smith & Nephew, Andover, MA) is a tool used to analyze patient-specific CT images. After automatic 3D rendering of the hip, dynamic ROM can be analyzed and areas of bony impingement defined on both the proximal femur and acetabular rim/pelvis. In addition, virtual surgical correction can be performed and dynamic impingement-free ROM reassessed. This tool also provides a platform for intra-operative assistance by performing virtual correction and creating an *in vivo* comparative

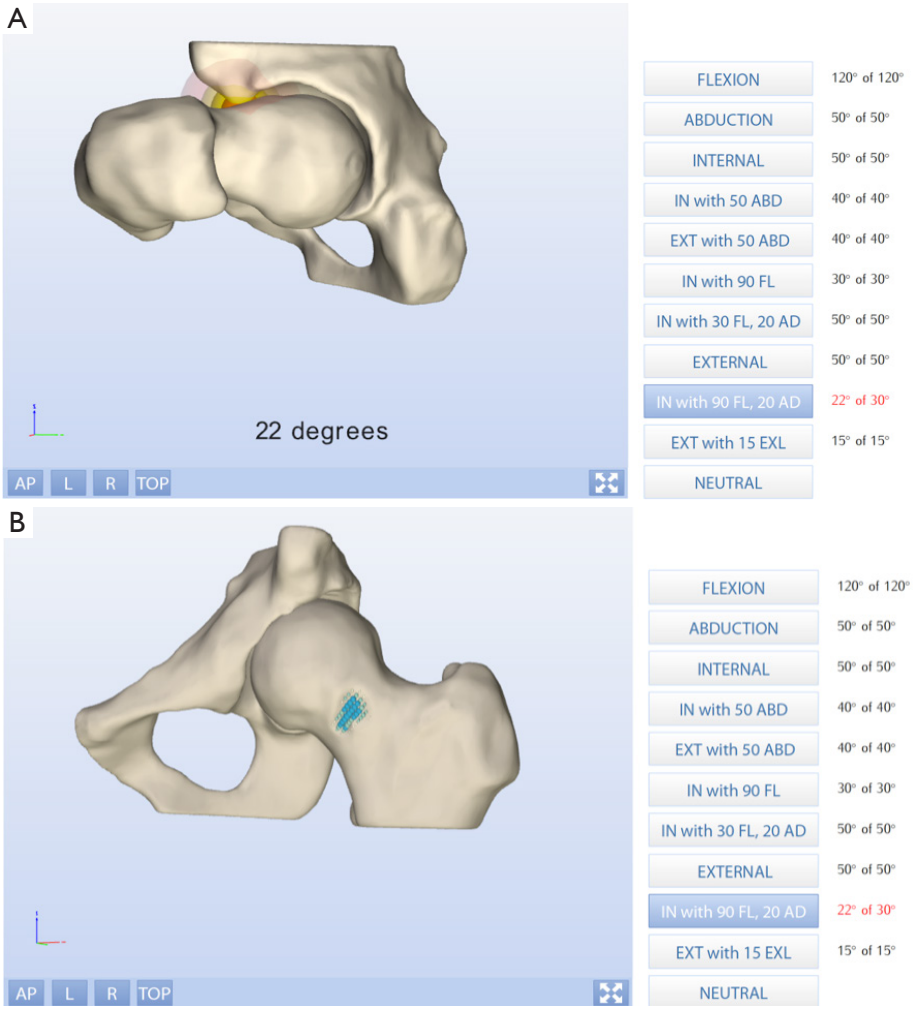

Figure 11 MRI based 3D modelling and dynamic virtual assessment. (A) Virtual ROM detects impingement areas at specific degrees of motion represented on the right. In this 30-year-old male with a cam deformity there was impingement noted at 22° of internal rotation with 90° of flexion and 20° adduction; (B) pre-operative planning allows depiction of areas of impingement on the virtual model (blue and green dots on the femoral head-neck junction).

virtual fluoroscopic image.

(IV) Hip Analysis/semi-AutSeg using "Articulis™" (Clinical Graphics, The Netherlands) has been validated and tested for reliability (30). Multiple studies have successfully used this software for research and clinical purposes in asymptomatic and symptomatic populations from CT and MRI data sets (22,23,99,100).

Computer-based navigation

3D imaging and computer navigation could play a major role in the planning of HPS. Furthermore, these advances could improve patient outcomes and lessen intra-operative and postoperative complications, such as under resection and over resection (88). For instance, it has been used in different hip pathologies, such has:

(I) FAI (88): a modified version of BrainLAB Hip-CT, which has primarily been used to assist with total hip arthroplasty (91) has been applied to arthroscopic FAI surgery. A C-arm adapter (Fluoro 3D, Vector Vision) can be used to synchronize the 3D CT dataset with intra-operative fluoroscopy allowing real-time feedback of surgical instrument

placement in relation to the FHN (101). Planning and conduction of navigated osteochondroplasty using a surgical milling device was feasible and accurate (91).

(II) PAO (89): Pflugi *et al.* used two measurement units attached to the pelvis and peri-acetabular fragment. Registration of the patient was obtained with a pre-operatively acquired SM (considering the anterior pelvic plane) and a specific device used to include that orientation in the reference coordinate system. After registration, the two sensors are applied and orientation is displayed. A patient-SM generated from a pre-operatively acquired 3D data-set is used to monitor in real-time the re-orientation of the peri-acetabular fragment to improve femoral coverage.

Real-time functional imaging

Biomechanical knowledge on hip impingement has been limited from research using intra-operative observation (13) and computer models (86,102). Real-time *in vivo* impingement under conditions of physiologic joint loading would be ideal and hopefully lead to an improved understanding of which hips and morphologies become symptomatic.

Open MRI with ROM testing *in vivo* has significant advantages compared to computer simulations, image-based model tracking, intra-operative observation, and *ex vivo* studies as it permits (103):

(I) Assessment of impingement in hips during functional postures;

(II) Evaluating the effect of posture and cam/pincer morphology size on clinically meaningful impingement;

(III) Visualization of differences in cam morphology "behavior" between symptomatic and non-symptomatic cohorts.

Having virtual simulations as a starting point, one can easily appreciate the advantage of combined *in vivo* imaging and real time functional analysis.

3D printing

A long way was seen from radiographs to 3D printing (3Dpr), but undoubtedly computerization of radiology and orthopedics is an inescapable fact. 3D imaging and printing might be a step forward for patient-centric tailored approach, from individual anatomy to treatment planning and building specific hardware needed for each patient (99). 3Dpr might be applied in subject-specific tools and surgical device building (100,104), as well as, in complex clinical settings such as pelvic osteotomies (105).

A combination of 3Dpr and CompAssist virtual surgical planning has also been used for pre-operative planning of acetabular fracture reduction (106). The authors stated that 3Dpr technology combined with virtual surgery for acetabular fractures is feasible, accurate, and effective leading to improved patient-specific pre-operative planning and outcome of real surgery.

Future trends in MSK radiology

MRI in 2050

In brief, the future of MRI will include comprehensive 3D joint imaging, done within fractions of the time currently spent and multiparametric in nature, allowing for automated biochemical cartilage analysis. Undoubtedly MRI trends include:

(I) Field strengths greater than 3.0 Tesla will be the new standard;

(II) 3D MRI acquisitions with potential for secondary multiplanar reconstructions performed in any desired sequence weighting;

(III) hR non-contrast imaging will replace MRA, with improved hR 3D cartilage assessment;

(IV) Implementation of quantitative imaging biomarkers in clinical routine imaging;

(V) Semiautomated or fully automated diagnostic examinations (with the aid of artificial intelligence algorithms to diagnose and automatically quantify specific parameters).

Magnetic resonance fingerprinting (MRF) (107)

MRF uses a pseudorandomized acquisition that prompts the characteristics from different tissues to have a unique signal or "fingerprint" that is dependent of the unique multi-dimensional material properties under analysis. This technique permits a noninvasive quantification of multiple properties of a material or tissue simultaneously through a new approach to data acquisition, post-processing and visualization. These can then be translated into quantitative maps of the MR parameters of interest. This technique would be useful to:

(I) Provide a novel approach to analyze, quantify and diagnose simple and complex changes that can represent disease surrogates on early/preventable disease;
(II) Accurately identify the presence of targeted molecules/tissue-specific material, which will increase the diagnostic and prognostic capability of MRI;
(III) Substantially decrease measurement errors and improve accuracy when coupled with a specific pattern recognition algorithm.

Big data and artificial intelligence

Understanding the advantages and limitations associated with large databases, particularly in the era of value-based health care is paramount. The implementation of standardized national orthopedic registries in conjunction with readily programmable and adaptable programs tailored to radiologists and orthopedic surgeons will ultimately improve patient outcomes while minimizing the economic burden (108,109).

One promising new technology with the potential to launch the next stage of progress in medical image is artificial intelligence (AI), which is the science of engineering intelligent machines and computer programs. Machine learning (ML) derives from AI and is defined as a set of methods that automatically detect patterns in data, and then utilize those patterns to predict future data or enable decision making under uncertain conditions (110). Applications in medical imaging include (111) (I) automatic labeling and captioning; (II) image segmentation and registration; (III) computer-aided detection and diagnosis; (IV) acting as a reading assistant and automatic dictation; (V) integration with healthcare big data.

Personalized medicine and biobanks

Personalized medicine will transform radiology and the health system within the next 50 years. The original concept of precision medicine involves the prevention and implementation of treatment strategies that consider individual variability by assessing large sets of data, including patient information, medical imaging, and genomic sequences (112). Patient-based imaging data will be implemented and cross-linked to population based–data already acquired in biobanks. These biological databanks are designed to identify early environmental and genetic causes of normal and abnormal growth, development and health from fetal life until young adulthood. They are already well underway and established as a comprehensive population-based health knowledge (112).

Conclusions

Technological innovation was essential for the recent transformation of MSK imaging. State-of-the-art contemporary joint imaging has allowed for improved diagnostic accuracy of most conditions that affect the hip and surrounding structures. Imaging the hip in the future will permit an ultra-fast, near perfect, noninvasive automated quantification of clinically relevant bone and soft tissue pathology through data acquisition, post-processing and visualization. Conceptually, this will involve a personalized approach and population-specific matching to standardize data from healthy and diseased individuals.

Acknowledgments

The authors would like to thank José Roquette, João Sá, Isabel Vaz and Pedro Patrício for their continuing and enthusiastic support of clinical research at Hospital da Luz.
Funding: None.

Footnote

Provenance and Peer Review: This article was commissioned by the Guest Editors (Olufemi R. Ayeni and Ryan P. Coughlin) for the series "Future Perspectives in Hip Preservation and Arthroscopy" published in *Annals of Joint*. The article has undergone external peer.

Conflicts of Interest: Both authors have completed the ICMJE uniform disclosure form (available at http://dx.doi.org/10.21037/aoj.2018.04.10). The series "Future Perspectives in Hip Preservation and Arthroscopy" was commissioned by the editorial office without any funding or sponsorship. The authors have no other conflicts of interest to declare.

Ethical Statement: The authors are accountable for all aspects of the work in ensuring that questions related to the accuracy or integrity of any part of the work are appropriately investigated and resolved.

References

1. Oei EH, van Tiel J, Robinson WH et al. Quantitative radiologic imaging techniques for articular cartilage composition: toward early diagnosis and development of disease-modifying therapeutics for osteoarthritis. Arthritis Care Res (Hoboken) 2014;66:1129-41.
2. Sutter R, Zanetti M, Pfirrmann CWA. New Developments in Hip Imaging. Radiology 2012;264:651-67.
3. McEnery KW, Wilson AJ, Murphy WA. Comparison of spiral computed tomography versus conventional computed tomography multiplanar reconstructions of a fracture displacement phantom. Invest Radiol 1994;29:665-70.
4. Elmslie RC. Remarks on aetiological factors in osteo-arthritis of the hip-joint. Br Med J 1933;1:1-46.1.
5. Wiles P. The surgery of the osteo-arthritic hip. Clin Orthop Relat Res 2003;(417):3-16.
6. Murray RO. The aetiology of primary osteoarthritis of the hip. Br J Radiol 1965;38:810-24.
7. Ambrose J. Computerized transverse axial scanning (tomography). 2. Clinical application. Br J Radiol 1973;46:1023-47.
8. Hounsfield GN. Computerized transverse axial scanning (tomography). 1. Description of system. Br J Radiol 1973;46:1016-22.
9. Stulberg SDC, Harris LD, Ramsey WH, et al. Unrecognized childhood hip disease: a major cause of idiopathic osteoarthritis of the hip. The hip Proceedings of the third open scientific meetings of the hip society 1975.
10. Mansfield P, Maudsley AA. Medical imaging by NMR. Br J Radiol 1977;50:188-94.
11. Hajek PC, Baker LL, Sartoris DJ, et al. MR arthrography: anatomic-pathologic investigation. Radiology 1987;163:141-7.
12. Langen HJ, Klein HM, Wein B, et al. Comparative evaluation of digital radiography versus conventional radiography of fractured skulls. Invest Radiol 1993;28:686-9.
13. Ganz R, Gill TJ, Gautier E, et al. Surgical dislocation of the adult hip a technique with full access to the femoral head and acetabulum without the risk of avascular necrosis. J Bone Joint Surg Br 2001;83:1119-24.
14. Polak JF, Jolesz FA, Adams DF. Magnetic resonance imaging of skeletal muscle. Prolongation of T1 and T2 subsequent to denervation. Invest Radiol 1988;23:365-9.
15. Hodler J, Yu JS, Goodwin D, et al. MR arthrography of the hip: improved imaging of the acetabular labrum with histologic correlation in cadavers. AJR Am J Roentgenol 1995;165:887-91.
16. Ganz R, Parvizi J, Beck M, et al. Femoroacetabular impingement: a cause for osteoarthritis of the hip. Clin Orthop Relat Res 2003;(417):112-20.
17. Riley GM, McWalter EJ, Stevens KJ, et al. MRI of the Hip for the evaluation of femoroacetabular impingement; past, present, and future. J Magn Reson Imaging 2015;41:558-72.
18. Khan M, Bedi A, Fu F, et al. New perspectives on femoroacetabular impingement syndrome. Nat Rev Rheumatol 2016;12:303-10.
19. Thomas GE, Palmer AJ, Batra RN, et al. Subclinical deformities of the hip are significant predictors of radiographic osteoarthritis and joint replacement in women. A 20 year longitudinal cohort study. Osteoarthritis Cartilage 2014;22:1504-10.
20. Agricola R, Weinans H. Femoroacetabular impingement: what is its link with osteoarthritis? Br J Sports Med 2016;50:957-8.
21. Li AE, Jawetz ST, Greditzer HG 4th, et al. MRI Evaluation of Femoroacetabular Impingement After Hip Preservation Surgery. AJR Am J Roentgenol 2016;207:392-400.
22. Khodarahmi I, Fritz J. Advanced MR Imaging after Total Hip Arthroplasty: The Clinical Impact. Semin Musculoskelet Radiol 2017;21:616-29.
23. Sutter R, Stoel BC, Buck FM, et al. Internal Derangements of Joints-Past, Present, and Future. Invest Radiol 2015;50:601-14.
24. Ganz R, Leunig M, Leunig-Ganz K, et al. The Etiology of Osteoarthritis of the Hip. Clin Orthop Relat Res 2008;466:264-72.
25. Sutter R, Pfirrmann CWA. Update on Femoroacetabular Impingement: What Is New, and How Should We Assess It? Semin Musculoskelet Radiol 2017;21:518-28.
26. Li AE, Jawetz ST, Greditzer HG, et al. MRI for the preoperative evaluation of femoroacetabular impingement. Insights Imaging. Insights Imaging

2016;7:187-98.
27. Griffin DR, Dickenson EJ, O'Donnell J, et al. The Warwick Agreement on femoroacetabular impingement syndrome (FAI syndrome): an international consensus statement. Br J Sports Med 2016;50:1169-76.
28. Khan W, Khan M, Alradwan H, et al. Utility of Intra-articular Hip Injections for Femoroacetabular Impingement: A Systematic Review. Orthop J Sports Med 2015;3:2325967115601030.
29. Buck FM, Hodler J, Zanetti M, et al. Ultrasound for the evaluation of femoroacetabular impingement of the cam type. Diagnostic performance of qualitative criteria and alpha angle measurements. Eur Radiol 2011;21:167-75.
30. Röling MA, Visser MI, Oei EHG, et al. A quantitative non-invasive assessment of femoroacetabular impingement with CT-based dynamic simulation--cadaveric validation study. BMC Musculoskelet Disord 2015;16:50.
31. Weber AE, Jacobson JA, Bedi A. A review of imaging modalities for the hip. Curr Rev Musculoskelet Med 2013;6:226-34.
32. Kraeutler MJ, Chadayammuri V, Garabekyan T, et al. Femoral Version Abnormalities Significantly Outweigh Effect of Cam Impingement on Hip Internal Rotation. J Bone Joint Surg Am 2018;100:205-10.
33. Mascarenhas VV, Rego P, Dantas P, et al. Cam deformity and the omega angle, a novel quantitative measurement of femoral head-neck morphology: a 3D CT gender analysis in asymptomatic subjects. Eur Radiol 2017;27:2011-23.
34. Bittersohl B, Steppacher S, Haamberg T, et al. Cartilage damage in femoroacetabular impingement (FAI): preliminary results on comparison of standard diagnostic vs delayed gadolinium-enhanced magnetic resonance imaging of cartilage (dGEMRIC). Osteoarthritis Cartilage 2009;17:1297-306.
35. Krych AJ, King AH, Berardelli RL, et al. Is Subchondral Acetabular Edema or Cystic Change on MRI a Contraindication for Hip Arthroscopy in Patients With Femoroacetabular Impingement? Am J Sports Med 2016;44:454-9.
36. Gold SL, Burge AJ, Potter HG. MRI of hip cartilage: joint morphology, structure, and composition. Clin Orthop Relat Res 2012;470:3321-31.
37. Ai T, Morelli JN, Hu X, et al. A historical overview of magnetic resonance imaging, focusing on technological innovations. Invest Radiol 2012;47:725-41.
38. Tao H, Shang X, Lu R, et al. Quantitative magnetic resonance imaging (MRI) evaluation of cartilage repair after microfracture (MF) treatment for adult unstable osteochondritis dissecans (OCD) in the ankle: correlations with clinical outcome. Eur Radiol 2014;24:1758-67.
39. Wang L, Wu Y, Chang G, et al. Rapid isotropic 3D-sodium MRI of the knee joint in vivo at 7T. J Magn Reson Imaging 2009;30:606-14.
40. Palmer A, Fernquest S, Rombach I, et al. Diagnostic and prognostic value of delayed Gadolinium Enhanced Magnetic Resonance Imaging of Cartilage (dGEMRIC) in early osteoarthritis of the hip. Osteoarthritis Cartilage 2017;25:1468-77.
41. Oei EH. Quantitative musculoskeletal imaging biomarkers. Quant Imaging Med Surg 2016;6:621-2.
42. Kuo R, Panchal M, Tanenbaum L, et al. 3.0 Tesla imaging of the musculoskeletal system. J Magn Reson Imaging 2007;25:245-61.
43. Shapiro L, Harish M, Hargreaves B, et al. Advances in musculoskeletal MRI: Technical considerations. J Magn Reson Imaging 2012;36:775-87.
44. Potter HG, Schachar J. High resolution noncontrast MRI of the hip. J Magn Reson Imaging 2010;31:268-78.
45. Ghebontni L, Roger B, El-khoury J, et al. MR arthrography of the hip: normal intra-articular structures and common disorders. Eur Radiol 2000;10:83-8.
46. Petchprapa CN, Rybak LD, Dunham KS, et al. Labral and cartilage abnormalities in young patients with hip pain: accuracy of 3-Tesla indirect MR arthrography. Skeletal Radiol 2015;44:97-105.
47. Leunig M, Podeszwa D, Beck M, et al. Magnetic resonance arthrography of labral disorders in hips with dysplasia and impingement. Clin Orthop Relat Res 2004;(418):74-80.
48. Perdikakis E, Karachalios T, Katonis P, et al. Comparison of MR-arthrography and MDCT-arthrography for detection of labral and articular cartilage hip pathology. Skeletal Radiol 2011;40:1441-7.
49. Smith TO, Hilton G, Toms AP, et al. The diagnostic accuracy of acetabular labral tears using magnetic resonance imaging and magnetic resonance arthrography: a meta-analysis. Eur Radiol 2011;21:863-74.
50. Waldt S, Burkart A, Lange P, et al. Diagnostic performance of MR arthrography in the assessment of superior labral anteroposterior lesions of the shoulder. AJR Am J Roentgenol 2004;182:1271-8.
51. Cerezal L, Carro LP, Llorca J, et al. Usefulness of MR arthrography of the hip with leg traction in the evaluation of ligamentum teres injuries. Skeletal Radiol 2015;44:1585-95.

52. Saied AM, Redant C, El-Batouty M, et al. Accuracy of magnetic resonance studies in the detection of chondral and labral lesions in femoroacetabular impingement: systematic review and meta-analysis. BMC Musculoskelet Disord 2017;18:83.
53. Sutter R, Zubler V, Hoffmann A, et al. Hip MRI: How Useful Is Intraarticular Contrast Material for Evaluating Surgically Proven Lesions of the Labrum and Articular Cartilage? AJR Am J Roentgenol 2014;202:160-9.
54. Llopis E, Cerezal L, Kassarjian A, et al. Direct MR arthrography of the hip with leg traction: feasibility for assessing articular cartilage. AJR Am J Roentgenol 2008;190:1124-8.
55. Schmaranzer F, Klauser A, Kogler M, et al. Diagnostic performance of direct traction MR arthrography of the hip: detection of chondral and labral lesions with arthroscopic comparison. Eur Radiol 2015;25:1721-30.
56. Schmid MR, Nötzli HP, Zanetti M, et al. Cartilage lesions in the hip: diagnostic effectiveness of MR arthrography. Radiology 2003;226:382-6.
57. Neumann G, Mendicuti AD, Zou KH, et al. Prevalence of labral tears and cartilage loss in patients with mechanical symptoms of the hip: evaluation using MR arthrography. Osteoarthritis Cartilage 2007;15:909-17.
58. Bittersohl B, Hosalkar HS, Hesper T, et al. Advanced Imaging in Femoroacetabular Impingement: Current State and Future Prospects. Front Surg 2015;2:34.
59. Mamisch TC, Kain MSH, Bittersohl B, et al. Delayed gadolinium-enhanced magnetic resonance imaging of cartilage (dGEMRIC) in Femoacetabular impingement. J Orthop Res 2011;29:1305-11.
60. Domayer SE, Mamisch TC, Kress I, et al. Radial dGEMRIC in developmental dysplasia of the hip and in femoroacetabular impingement: preliminary results. Osteoarthritis Cartilage 2010;18:1421-8.
61. Bittersohl B, Hosalkar HS, Apprich S, et al. Comparison of pre-operative dGEMRIC imaging with intra-operative findings in femoroacetabular impingement: preliminary findings. Skeletal Radiol 2011;40:553-61.
62. Guermazi A, Alizai H, Crema MD, et al. Compositional MRI techniques for evaluation of cartilage degeneration in osteoarthritis. Osteoarthritis Cartilage 2015;23:1639-53.
63. Zilkens C, Miese F, Krauspe R, et al. Symptomatic Femoroacetabular Impingement: Does the Offset Decrease Correlate With Cartilage Damage? A Pilot Study. Clin Orthop Relat Res 2013;471:2173-82.
64. Anwander H, Rakhra KS, Melkus G, et al. T1q Hip Cartilage Mapping in Assessing Patients With Cam Morphology: How Can We Optimize the Regions of Interest? Clin Orthop Relat Res 2017;475:1066-75.
65. Subburaj K, Valentinitsch A, Dillon AB, et al. Regional variations in MR relaxation of hip joint cartilage in subjects with and without femoralacetabular impingement. Magn Reson Imaging 2013;31:1129-36.
66. van Tiel J, Kotek G, Reijman M, et al. Is T1ρ Mapping an Alternative to Delayed Gadolinium-enhanced MR Imaging of Cartilage in the Assessment of Sulphated Glycosaminoglycan Content in Human Osteoarthritic Knees? An in Vivo Validation Study. Radiology 2016;279:523-31.
67. Watanabe A, Boesch C, Siebenrock K, et al. T2 mapping of hip articular cartilage in healthy volunteers at 3T: a study of topographic variation. J Magn Reson Imaging 2007;26:165-71.
68. Nishii T, Shiomi T, Tanaka H, et al. Loaded Cartilage T2 Mapping in Patients with Hip Dysplasia. Radiology 2010;256:955-65.
69. Yamamoto S, Watanabe A, Nakamura J, et al. Quantitative T2 mapping of femoral head cartilage in systemic lupus erythematosus patients with noncollapsed osteonecrosis of the femoral head associated with corticosteroid therapy. J Magn Reson Imaging 2011;34:1151-8.
70. Hesper T, Neugroda C, Schleich C et al. T2*-Mapping of Acetabular Cartilage in Patients With Femoroacetabular Impingement at 3 Tesla: Comparative Analysis with Arthroscopic Findings. Cartilage 2018;9:118-26.
71. Bittersohl B, Hosalkar HS, Hughes T, et al. Feasibility of T2*mapping for the evaluation of hip joint cartilage at 1.5T using a three-dimensional (3D), gradient-echo (GRE) sequence: A prospective study. Magn Reson Med 2009;62:896-901.
72. Bittersohl B, Miese FR, Hosalkar HS, et al. T2* mapping of acetabular and femoral hip joint cartilage at 3 T: a prospective controlled study. Invest Radiol 2012;47:392-7.
73. Apprich S, Mamisch TC, Welsch GH, et al. Evaluation of articular cartilage in patients with femoroacetabular impingement (FAI) using T2* mapping at different time points at 3.0 Tesla MRI: a feasibility study. Skeletal Radiol 2012;41:987-95.
74. Siebenrock KA, Kienle KP, Steppacher SD, et al. Biochemical MRI Predicts Hip Osteoarthritis in an Experimental Ovine Femoroacetabular Impingement Model. Clin Orthop Relat Res 2015;473:1318-24.
75. Zilkens C, Miese F, Kim YJ, et al. Direct comparison of intra-articular versus intravenous delayed gadolinium-enhanced MRI of hip joint cartilage. J Magn Reson

Imaging 2014;39:94-102.
76. Zilkens C, Tiderius CJ, Krauspe R, et al. Current knowledge and importance of dGEMRIC techniques in diagnosis of hip joint diseases. Skeletal Radiol 2015;44:1073-83.
77. Lattanzi R, Petchprapa C, Glaser C, et al. A new method to analyze dGEMRIC measurements in femoroacetabular impingement: preliminary validation against arthroscopic findings. Osteoarthritis Cartilage 2012;20:1127-33.
78. Liu Q, Wang W, Thoreson AR, et al. Finite element prediction of contact pressures in cam-type femoroacetabular impingement with varied alpha angles. Comput Methods Biomech Biomed Engin 2017;20:294-301.
79. Matzat SJ, van Tiel J, Gold GE, et al. Quantitative MRI techniques of cartilage composition. Quant Imaging Med Surg 2013;3:162-74.
80. Hesper T, Hosalkar HS, Bittersohl D, et al. T2* mapping for articular cartilage assessment: principles, current applications, and future prospects. Skeletal Radiol 2014;43:1429-45.
81. Nozaki T, Kaneko Y, Yu HJ, et al. T1rho mapping of entire femoral cartilage using depth- and angle-dependent analysis. Eur Radiol 2016;26:1952-62.
82. Ling W, Regatte RR, Navon G, et al. Assessment of glycosaminoglycan concentration in vivo by chemical exchange-dependent saturation transfer (gagCEST). Proc Natl Acad Sci U S A 2008;105:2266-70.
83. Binks DA, Hodgson RJ, Ries ME, et al. Quantitative parametric MRI of articular cartilage: a review of progress and open challenges. Br J Radiol 2013;86:20120163.
84. Bangerter NK, Tarbox GJ, Taylor MD, et al. Quantitative sodium magnetic resonance imaging of cartilage, muscle, and tendon. Quant Imaging Med Surg 2016;6:699-714.
85. Xia Y, Fripp J, Chandra SS, et al. Automated 3D quantitative assessment and measurement of alpha angles from the femoral head-neck junction using MR imaging. Phys Med Biol 2015;60:7601-16.
86. Tannast M, Kubiak-Langer M, Langlotz F, et al. Noninvasive three-dimensional assessment of femoroacetabular impingement. J Orthop Res 2007;25:122-31.
87. Albers CE, Wambeek N, Hanke MS. Imaging of femoroacetabular impingement-current concepts. J Hip Preserv Surg 2016;3:245-61.
88. Albers CE, Hanke MS, Ecker TM, et al. Computer Assisted Diagnosis and Treatment Planning of Femoroacetabular Impingement (FAI). In: Lecture Notes in Computational Vision and Biomechanics. Cham: Springer International Publishing, 2015:173-96.
89. Pflugi S, Liu L, Ecker TM, et al. A cost-effective surgical navigation solution for periacetabular osteotomy (PAO) surgery. Int J Comput Assist Radiol Surg 2016;11:271-80.
90. Kuhn AW, Ross JR, Bedi A. Three-dimensional Imaging and Computer Navigation in Planning for Hip Preservation Surgery. Sports Med Arthrosc 2015;23:e31-8.
91. Ecker TM, Puls M, Steppacher SD, et al. Computer-assisted femoral head-neck osteochondroplasty using a surgical milling device an in vitro accuracy study. J Arthroplasty 2012;27:310-6.
92. Schumann S, Liu L, Tannast M, et al. An Integrated System for 3D Hip Joint Reconstruction from 2D X-rays: A Preliminary Validation Study. Ann Biomed Eng 2013;41:2077-87.
93. Xia Y, Fripp J, Chandra SS, et al. Automated bone segmentation from large field of view 3D MR images of the hip joint. Phys Med Biol 2013;58:7375-90.
94. Audenaert EA, Baelde N, Huysse W, et al. Development of a three-dimensional detection method of cam deformities in femoroacetabular impingement. Skeletal Radiol 2011;40:921-7.
95. Masjedi M, Azimi DY, Nightingale CL, et al. A method of assessing the severity of cam type femoro-acetabular impingement in three dimensions. Hip Int 2012;22:677-82.
96. Chandra SS, Xia Y, Engstrom C, et al. Focused shape models for hip joint segmentation in 3D magnetic resonance images. Med Image Anal 2014;18:567-78.
97. Heimann T, Meinzer HP. Statistical shape models for 3D medical image segmentation: a review. Med Image Anal 2009;13:543-63.
98. Chu C, Chen C, Liu L, et al. FACTS: Fully Automatic CT Segmentation of a Hip Joint. Ann Biomed Eng 2015;43:1247-59.
99. Flecher X, Migaud H. From radiographs to 3D printing: How can new surgical planning technologies contribute to hip surgery? Orthop Traumatol Surg Res 2017;103:323-4.
100. Rankin TM, Giovinco NA, Cucher DJ, et al. Three-dimensional printing surgical instruments: are we there yet? J Surg Res 2014;189:193-7.
101. Brunner A, Horisberger M, Herzog RF. Evaluation of a computed tomography-based navigation system prototype for hip arthroscopy in the treatment of femoroacetabular cam impingement. Arthroscopy 2009;25:382-91.

102. Khanduja V, Baelde N, Dobbelaere A, et al. Patient-specific assessment of dysmorphism of the femoral head-neck junction: a statistical shape model approach. Int J Med Robot 2016;12:765-72.
103. Buchan LL, Zhang H, Konan S, et al. Open-MRI measures of cam intrusion for hips in an anterior impingement position relate to acetabular contact force. J Orthop Res 2016;34:205-16.
104. Brown GA, Milner B, Firoozbakhsh K. Application of computer-generated stereolithography and interpositioning template in acetabular fractures: a report of eight cases. J Orthop Trauma 2002;16:347-52.
105. Upex P, Jouffroy P, Riouallon G. Application of 3D printing for treating fractures of both columns of the acetabulum: Benefit of pre-contouring plates on the mirrored healthy pelvis. Orthop Traumatol Surg Res 2017;103:331-4.
106. Zeng C, Xing W, Wu Z, et al. A combination of three-dimensional printing and computer-assisted virtual surgical procedure for preoperative planning of acetabular fracture reduction. Injury 2016;47:2223-7.
107. Ma D, Gulani V, Seiberlich N, et al. Magnetic resonance fingerprinting. Nature 2013;495:187-92.
108. Anoushiravani AA, Patton J, Sayeed Z, et al. Big Data, Big Research: Implementing Population Health-Based Research Models and Integrating Care to Reduce Cost and Improve Outcomes. Orthop Clin North Am 2016;47:717-24.
109. Aphinyanaphongs Y. Big Data Analyses in Health and Opportunities for Research in Radiology. Semin Musculoskelet Radiol 2017;21:32-6.
110. Mayo RC, Leung J. Artificial intelligence and deep learning - Radiology's next frontier? Clin Imaging 2017;49:87-8.
111. Lee JG, Jun S, Cho YW, et al. Deep Learning in Medical Imaging: General Overview. Korean J Radiol 2017;18:570-84.
112. Kooijman MN, Kruithof CJ, van Duijn CM, et al. The Generation R Study: design and cohort update 2017. Eur J Epidemiol 2016;31:1243-64.

doi: 10.21037/aoj.2018.04.10
Cite this article as: Mascarenhas VV, Caetano A. Imaging the young adult hip in the future. Ann Joint 2018;3:47.